Published for SISSA by Springer

Received: May 11, 2017
Revised: June 16, 2017
Accepted: June 24, 2017
Published: July 4, 2017

Muon specific two-Higgs-doublet model

Tomohiro Abe,[a,b] **Ryosuke Sato**[c] **and Kei Yagyu**[d]

[a] *Institute for Advanced Research, Nagoya University, Furo-cho Chikusa-ku, Nagoya, Aichi, 464-8602 Japan*

[b] *Kobayashi-Maskawa Institute for the Origin of Particles and the Universe, Nagoya University, Furo-cho Chikusa-ku, Nagoya, Aichi, 464-8602 Japan*

[c] *Department of Particle Physics and Astrophysics, Weizmann Institute of Science, Rehovot 7610001, Israel*

[d] *INFN, Sezione di Firenze, and Department of Physics and Astronomy, University of Florence, Via G. Sansone 1, 50019 Sesto Fiorentino, Italy*

E-mail: abetomo@kmi.nagoya-u.ac.jp, ryosuke.sato@weizmann.ac.il, yagyu@fi.infn.it

Abstract: We investigate a new type of a two-Higgs-doublet model as a solution of the muon $g-2$ anomaly. We impose a softly-broken Z_4 symmetry to forbid tree level flavor changing neutral currents in a natural way. This Z_4 symmetry restricts the structure of Yukawa couplings. As a result, extra Higgs boson couplings to muons are enhanced by a factor of $\tan\beta$, while their couplings to all the other standard model fermions are suppressed by $\cot\beta$. Thanks to this coupling property, we can avoid the constraint from leptonic τ decays in contrast to the lepton specific two-Higgs-doublet model, which can explain the muon $g-2$ within the 2σ level but cannot within the 1σ level due to this constraint. We find that the model can explain the muon $g-2$ within the 1σ level satisfying constraints from perturbative unitarity, vacuum stability, electroweak precision measurements, and current LHC data.

Keywords: Beyond Standard Model, Higgs Physics

ArXiv ePrint: 1705.01469

https://doi.org/10.1007/JHEP07(2017)012

JHEP07(2017)012

Contents

JHEP07(2017)012

1 Introduction

It is well known that the measured value of the muon anomalous magnetic moment $(g-2)$ [1] deviates from the standard model (SM) prediction [2, 3] with more than 3σ. This large deviation has been a long standing problem in particle physics, and many models beyond the SM have been studied to solve this discrepancy [4]. Since the new experiments are planed at Fermilab [5] and J-PARC [6], it is worthwhile to find a good benchmark model that solves this problem. Among various scenarios, the lepton specific (Type-X) two-Higgs-doublet model (THDM) gives a simple solution to explain the muon $g-2$ anomaly [7–9].[1] This model is known as one of the four THDMs [10–12] with a softly-broken Z_2 symmetry which is imposed to avoid flavor changing neutral currents (FCNCs) at the tree level [13]. This model contains additional Higgs bosons, namely a CP-even (H^0), a CP-odd (A^0), and charged ($H^\pm$) Higgs bosons. Their couplings to the SM charged leptons are enhanced by a factor of $\tan\beta$ which is the ratio of two Vacuum Expectation Values (VEVs) of the two doublet Higgs fields. Although this enhancement can significantly reduce the discrepancy

[1] Other scenarios of THDMs without the natural flavor conservation [13] are discussed in refs. [14–16].

	q_L^j	u_R^j	d_R^j	ℓ_L^e	ℓ_L^τ	ℓ_L^μ	e_R	τ_R	μ_R	H_1	H_2
$\mathrm{SU}(3)_c$	3	3	3	1	1	1	1	1	1	1	1
$\mathrm{SU}(2)_L$	2	1	1	2	2	2	1	1	1	2	2
$\mathrm{U}(1)_Y$	1/6	2/3	−1/3	−1/2	−1/2	−1/2	−1	−1	−1	1/2	1/2
Z_4	1	1	1	1	1	i	1	1	i	−1	1

Table 1. Particle contents and the charge assignment.

in the muon $g-2$, its amount is severely constrained from precision measurements of the leptonic τ decay: $\tau \to \mu\nu_\tau\bar{\nu}_\mu$ whose amplitude with the $H^\pm$ mediation is proportional to $\tan^2\beta$. Consequently, it turns out difficult to explain the muon $g-2$ anomaly within the 1σ level [17, 18].

In this paper, we propose a new type of the THDM that avoids the constraint from the τ decay without losing the advantage of the Type-X THDM. We impose a softly-broken Z_4 symmetry to forbid tree level FCNCs in a natural way as in the Type-X THDM. This Z_4 symmetry is also important to restrict the structure of Yukawa couplings. As a result, only the additional Higgs boson couplings to muons are enhanced by a factor of $\tan\beta$, while their couplings to all the other SM fermions are suppressed by $\cot\beta$. We call this model the "muon specific THDM (μTHDM)". Thanks to this coupling property, the large contribution to the leptonic τ decay amplitude by $\tan^2\beta$ provided in the Type-X THDM disappears in the μTHDM because of the cancellation of the $\tan\beta$ factor between the tau and the muon Yukawa couplings to $H^\pm$. This is a crucial difference of this model from the Type-X THDM. We will show that the μTHDM can explain the muon $g-2$ anomaly within the 1σ level in the parameter space allowed by bounds from perturbative unitarity, vacuum stability, electroweak precision measurements, and current LHC data.

This paper is organized as follows. After describing our model in section 2, we discuss constraints on model parameters from perturbative unitarity, vacuum stability, electroweak precision measurements, and current LHC data in section 3. In addition, we show that the parameter space which explains the muon $g-2$ anomaly within 1σ is allowed by these constraints We devote section 4 for our conclusion.

2 Model

2.1 Lagrangian

The Higgs sector of the μTHDM is composed of two $\mathrm{SU}(2)_L$ doublet scalar fields H_1 and H_2. We impose a softly-broken Z_4 symmetry to prevent tree level FCNCs. The charge assignment for the SM fermions and the Higgs fields are summarized in table 1.[2]

[2]Our model can be extended so as to realize non-zero masses of left-handed neutrinos and large mixing angles between ν_μ and $\nu_{e,\tau}$ which are observed by neutrino experiments. We discuss such extension without a hard breaking of the Z_4 symmetry in appendix A.

JHEP07(2017)012

The Yukawa interaction terms under this charge assignment are given by[3]

$$\mathcal{L}^{\text{Yukawa}} = -\bar{q}_L \tilde{H}_2 Y_u u_R - \bar{q}_L H_2 Y_d d_R - \bar{L}_L H_1 Y_{\ell 1} E_R - \bar{L}_L H_2 Y_{\ell 2} E_R + (\text{h.c.}), \tag{2.1}$$

where $\tilde{H}_2 = i\sigma^2 H_2^*$, and Y_u, Y_d, $Y_{\ell 1}$ and $Y_{\ell 2}$ are 3×3 matrices in generation space. The left(right)-handed lepton filed L_L (E_R) is defined as

$$L_L = (\ell_L^e, \ell_L^\tau, \ell_L^\mu)^T, \quad E_R = (e_R, \tau_R, \mu_R)^T. \tag{2.2}$$

The Z_4 symmetry restricts the structure of the lepton Yukawa matrices as follows:

$$Y_{\ell 1} = \begin{pmatrix} 0 & 0 & 0 \\ 0 & 0 & 0 \\ 0 & 0 & y_\mu \end{pmatrix}, \quad Y_{\ell 2} = \begin{pmatrix} y_e & y_{e\tau} & 0 \\ y_{\tau e} & y_\tau & 0 \\ 0 & 0 & 0 \end{pmatrix}. \tag{2.3}$$

We can take $y_{e\tau} = y_{\tau e} = 0$ by field rotations without loss of generality.

The Higgs potential takes the same form as in the THDM with a softly-broken Z_2 symmetry:

$$\begin{aligned} V = {} & m_1^2 H_1^\dagger H_1 + m_2^2 H_2^\dagger H_2 - \left(m_3^2 H_1^\dagger H_2 + (\text{h.c.}) \right) + \frac{\lambda_1}{2} (H_1^\dagger H_1)^2 + \frac{\lambda_2}{2} (H_2^\dagger H_2)^2 \\ & + \lambda_3 (H_1^\dagger H_1)(H_2^\dagger H_2) + \lambda_4 (H_1^\dagger H_2)(H_2^\dagger H_1) + \left(\frac{1}{2} \lambda_5 (H_1^\dagger H_2)^2 + (\text{h.c.}) \right), \end{aligned} \tag{2.4}$$

where m_1^2, m_2^2, λ_1, λ_2, λ_3, and λ_4 are real. In general, m_3^2 and λ_5 are complex, but we assume these two parameters to be real for simplicity, by which the Higgs potential is CP-invariant.

We parametrize the component fields of the Higgs doublets by

$$H_i = \begin{pmatrix} \pi_i^+ \\ \frac{1}{\sqrt{2}} \left(v_i + \sigma_i - i\pi_i^3 \right) \end{pmatrix}, \qquad (i = 1, 2), \tag{2.5}$$

where v_1 (v_2) is the VEV of the H_1 (H_2) field. It is convenient to express these two VEVs in terms of v and $\tan\beta$ defined by $v \equiv \sqrt{v_1^2 + v_2^2} \simeq (\sqrt{2} G_F)^{-1/2} \simeq 246\,\text{GeV}$ with G_F being the Fermi constant and $\tan\beta \equiv v_2/v_1$, respectively.[4] The mass eigenstates of the scalar bosons and their relation to the gauge eigenstates expressed in eq. (2.5) are given by the following rotations:

$$\begin{pmatrix} \pi_Z \\ A^0 \end{pmatrix} = \begin{pmatrix} \cos\beta & \sin\beta \\ -\sin\beta & \cos\beta \end{pmatrix} \begin{pmatrix} \pi_1^3 \\ \pi_2^3 \end{pmatrix}, \tag{2.6}$$

$$\begin{pmatrix} \pi_{W^\pm} \\ H^\pm \end{pmatrix} = \begin{pmatrix} \cos\beta & \sin\beta \\ -\sin\beta & \cos\beta \end{pmatrix} \begin{pmatrix} \pi_1^\pm \\ \pi_2^\pm \end{pmatrix}, \tag{2.7}$$

$$\begin{pmatrix} H^0 \\ h \end{pmatrix} = \begin{pmatrix} \cos\alpha & \sin\alpha \\ -\sin\alpha & \cos\alpha \end{pmatrix} \begin{pmatrix} \sigma_1 \\ \sigma_2 \end{pmatrix}, \tag{2.8}$$

[3] We discuss the possibility of other discrete symmetries which realize this Yukawa structure in appendix B.

[4] The exact relation between v and G_F is given in appendix C.

JHEP07(2017)012

where $\pi_{W^\pm}$ and π_Z are the Nambu-Goldstone bosons which are absorbed into the longitudinal component of the $W^\pm$ and Z bosons, respectively. We identify h as the discovered Higgs boson with a mass of 125 GeV at the LHC. The mixing angle α is expressed by the potential parameters as

$$\tan 2\alpha = \frac{2(v^2\lambda_{345} - M^2)\tan\beta}{v^2(\lambda_1 - \lambda_2\tan^2\beta) - M^2(1-\tan^2\beta)}, \tag{2.9}$$

where

$$\lambda_{345} \equiv \lambda_3 + \lambda_4 + \lambda_5, \quad M^2 \equiv \frac{1+t_\beta^2}{t_\beta} m_3^2. \tag{2.10}$$

The CP-conserving Higgs potential can then be described by the following 8 independent parameters:

$$m_{H^\pm},\ m_A,\ m_H,\ m_h,\ M^2,\ \alpha,\ \beta,\ v, \tag{2.11}$$

where $m_{H^\pm}$, m_A, m_H and m_h denote the masses of $H^\pm$, A^0, H^0 and h, respectively.

We introduce the following shorthand notations for the later convenience.

$$s_x = \sin x, \quad c_x = \cos x, \quad t_x = \tan x. \tag{2.12}$$

2.2 Yukawa couplings in large $\tan\beta$ regime

From eq. (2.1), we can extract interaction terms for the mass eigenstates of the Higgs bosons with the third generation fermions and the muon as follows:

$$\begin{aligned}\mathcal{L}_{\rm int} = &-\sum_{f=t,b,\tau}\frac{m_f}{v}\left[\left(s_{\beta-\alpha}+\frac{c_{\beta-\alpha}}{t_\beta}\right)\overline{f}fh + \left(c_{\beta-\alpha}-\frac{s_{\beta-\alpha}}{t_\beta}\right)\overline{f}fH^0 + 2i\frac{I_f}{t_\beta}\overline{f}\gamma_5 f A^0\right] \\ &- \frac{m_\mu}{v}\left[(s_{\beta-\alpha}-t_\beta c_{\beta-\alpha})\,\overline{\mu}\mu h + (c_{\beta-\alpha}+t_\beta s_{\beta-\alpha})\,\overline{\mu}\mu H^0 + it_\beta\overline{\mu}\gamma_5\mu A^0\right] \\ &- \frac{\sqrt{2}}{v}\left\{\frac{1}{t_\beta}\left[\overline{t}\,(m_b \mathrm{P}_R - m_t\,\mathrm{P}_L)\,b\,H^+ + m_\tau\overline{\nu_\tau}\,P_R\,\tau\,H^+\right] - t_\beta m_\mu\overline{\nu_\mu}\,P_R\,\mu\,H^+ + (\text{h.c.})\right\},\end{aligned} \tag{2.13}$$

where $P_L(P_R)$ is the projection operator for left(right)-handed fermions and $I_f = +1/2(-1/2)$ for $f = t\,(b,\tau,\mu)$. The masses of fermions are given by

$$m_\mu = \frac{v}{\sqrt{2}}\frac{y_\mu}{\sqrt{1+t_\beta^2}}, \quad m_f = \frac{v}{\sqrt{2}}\frac{y_f t_\beta}{\sqrt{1+t_\beta^2}} \quad (f = t,b,\tau)\,. \tag{2.14}$$

From eq. (2.13), it is clear that only the muon couplings to the extra Higgs bosons are enhanced by taking large $\tan\beta$.

In order to solve the muon $g-2$ anomaly, we need a large value of $\tan\beta$ to obtain significant loop effects of extra Higgs bosons as we will show it in the next section. Let us here discuss how large value of $\tan\beta$ we can take without spoiling perturbativity. From eq. (2.14) we obtain

$$y_\mu = \frac{\sqrt{2}m_\mu}{v}\sqrt{1+t_\beta^2} \simeq 0.6\left(\frac{t_\beta}{1000}\right). \tag{2.15}$$

JHEP07(2017)012

For example, $t_\beta \lesssim 5000$ for $y_\mu \lesssim 3$. Clearly from eq. (2.14), all the other Yukawa couplings approach to the corresponding SM value in large $\tan\beta$, so that they do not cause the violation of perturbativity in this limit.

2.3 Scalar quartic couplings in large $\tan\beta$ regime

Next, we discuss the behavior of the Higgs quartic couplings in the large $\tan\beta$ regime. All these couplings (times v^2) can be rewritten in terms of the parameters shown in eq. (2.11) as

$$\lambda_1 v^2 = \left(m_h^2 c_{\beta-\alpha}^2 + m_H^2 s_{\beta-\alpha}^2 - M^2\right) t_\beta^2 + 2(m_H^2 - m_h^2) s_{\beta-\alpha} c_{\beta-\alpha}\, t_\beta + m_h^2 s_{\beta-\alpha}^2 + m_H^2 c_{\beta-\alpha}^2, \tag{2.16}$$

$$\lambda_2 v^2 = m_h^2 s_{\beta-\alpha}^2 + m_H^2 c_{\beta-\alpha}^2 - 2(m_H^2 - m_h^2)\frac{c_{\beta-\alpha} s_{\beta-\alpha}}{t_\beta} + (m_h^2 c_{\beta-\alpha}^2 + m_H^2 s_{\beta-\alpha}^2 - M^2)\frac{1}{t_\beta^2}, \tag{2.17}$$

$$\lambda_3 v^2 = (m_H^2 - m_h^2) c_{\beta-\alpha} s_{\beta-\alpha}\left(t_\beta - \frac{1}{t_\beta}\right) + 2m_{H^\pm}^2 - M^2 + m_H^2 - m_h^2 (c_{\beta-\alpha}^2 - s_{\beta-\alpha}^2), \tag{2.18}$$

$$\lambda_4 v^2 = M^2 - m_A^2 - 2(m_{H^\pm}^2 - m_A^2), \tag{2.19}$$

$$\lambda_5 v^2 = M^2 - m_A^2. \tag{2.20}$$

We find that in the large $\tan\beta$ regime, λ_1 and λ_3 can be very large because they are proportional to t_β^2 and t_β, respectively, which causes the validity of perturbative calculations to be lost. In order to keep λ_1 and λ_3 to be reasonable values, we can take M^2 and $s_{\beta-\alpha}$ so as to cancel the large contribution from the t_β^2 and t_β terms as follows:

$$M^2 = m_h^2 c_{\beta-\alpha}^2 + m_H^2 s_{\beta-\alpha}^2 - 2 s_{\beta-\alpha} c_{\beta-\alpha}(m_h^2 - m_H^2)\frac{1}{t_\beta} - X v^2 \frac{1}{t_\beta^2}, \tag{2.21}$$

$$s_{\beta-\alpha} = 1, \tag{2.22}$$

where X is an arbitrary number.

It is worth noting that in the limit $s_{\beta-\alpha} \to 1$ (the so-called alignment limit [19]), the SM-like Higgs boson h couplings to weak bosons g_{hVV} $(V = W, Z)$ and fermions g_{hff} become the same value as those of the SM Higgs boson at the tree level, because these are given by $g_{hVV} = g_{hVV}^{\rm SM} s_{\beta-\alpha}$, $g_{hff} = g_{hff}^{\rm SM}(s_{\beta-\alpha} + c_{\beta-\alpha}/t_\beta)$ $(f \neq \mu)$ and $g_{h\mu\mu} = g_{h\mu\mu}^{\rm SM}(s_{\beta-\alpha} - c_{\beta-\alpha} t_\beta)$. Because no large deviation in the Higgs boson couplings from the SM prediction has been discovered at current LHC data [20], our choice $s_{\beta-\alpha} = 1$ is consistent with these results. After imposing eqs. (2.21) and (2.22), we find

$$\lambda_1 = \frac{m_h^2}{v^2} + X, \tag{2.23}$$

$$\lambda_2 = \frac{m_h^2}{v^2} + \frac{X}{t_\beta^4}, \tag{2.24}$$

$$\lambda_3 = \frac{2m_{H^\pm}^2 - 2m_H^2 + m_h^2}{v^2} + \frac{X}{t_\beta^2}, \tag{2.25}$$

$$\lambda_4 = \frac{m_H^2 + m_A^2 - 2m_{H^\pm}^2}{v^2} - \frac{X}{t_\beta^2}, \tag{2.26}$$

$$\lambda_5 = \frac{m_H^2 - m_A^2}{v^2} - \frac{X}{t_\beta^2}. \tag{2.27}$$

JHEP07(2017)012

These λ's are at most $\mathcal{O}(1)$ as long as we take $m^2_{H^\pm} \sim m^2_A \sim m^2_H$, so that we can still treat them as perturbation. We take $X = 0$ for simplicity in the following analysis. Constraints from perturbative unitarity is discussed in section 3.2.

3 Muon $g-2$ and constraints on parameter space

In this section, we discuss the muon $g-2$ anomaly and various constraints on the model parameters.

3.1 Muon $g-2$

In the scenario with $s_{\beta-\alpha} = 1$ as discussed in the previous section, new contributions to $a_\mu \equiv (g-2)/2$ purely comes from the loop contributions of H^0, A^0 and $H^\pm$, because the couplings of h becomes exactly the same as those of the SM Higgs boson at the tree level. One-loop diagram contributions to $\delta a_\mu \equiv a_\mu - a_\mu^{\rm SM}$ from additional Higgs boson loops are calculated as [21]

$$\delta a_\mu^H = \frac{G_F m_\mu^2}{4\sqrt{2}\pi^2} t_\beta^2 \left(\frac{c_{\beta-\alpha}}{t_\beta} + s_{\beta-\alpha}\right)^2 r_H f_H(r_H), \tag{3.1}$$

$$\delta a_\mu^A = \frac{G_F m_\mu^2}{4\sqrt{2}\pi^2} t_\beta^2 r_A f_A(r_A), \tag{3.2}$$

$$\delta a_\mu^{H^\pm} = \frac{G_F m_\mu^2}{4\sqrt{2}\pi^2} t_\beta^2 r_{H^\pm} f_{H^\pm}(r_{H^\pm}), \tag{3.3}$$

where $r_{H,A,H^\pm} = m_\mu^2/m^2_{H,A,H^\pm}$ and

$$f_H(r) = \int_0^1 dx \frac{x^2(2-x)}{rx^2 - x + 1}, \tag{3.4}$$

$$f_A(r) = \int_0^1 dx \frac{-x^3}{rx^2 - x + 1}, \tag{3.5}$$

$$f_{H^\pm}(r) = \int_0^1 dx \frac{-x^2(1-x)}{rx^2 + (1-r)x}. \tag{3.6}$$

For $r_{H,A,H^\pm} \ll 1$, we can approximate the above formulae as follows:

$$\delta a_\mu^H \simeq \frac{G_F m_\mu^2}{4\sqrt{2}\pi^2} t_\beta^2 \left(s_{\beta-\alpha} + \frac{c_{\beta-\alpha}}{t_\beta}\right)^2 \frac{m_\mu^2}{m_H^2}\left(-\frac{7}{6} - \ln\frac{m_\mu^2}{m_H^2}\right), \tag{3.7}$$

$$\delta a_\mu^A \simeq \frac{G_F m_\mu^2}{4\sqrt{2}\pi^2} \frac{m_\mu^2}{m_A^2}\left(\frac{11}{6} + \ln\frac{m_\mu^2}{m_A^2}\right), \tag{3.8}$$

$$\delta a_\mu^{H^\pm} \simeq \frac{G_F m_\mu^2}{4\sqrt{2}\pi^2} \frac{m_\mu^2}{m_{H^\pm}^2}\left(-\frac{1}{6}\right). \tag{3.9}$$

We here briefly mention the contribution from two-loop Barr-Zee diagrams [22, 23]. In the Type-II and Type-X THDMs, the Barr-Zee diagrams also give important contributions, because the tau and/or bottom Yukawa couplings to the additional Higgs bosons can be

JHEP07(2017)012

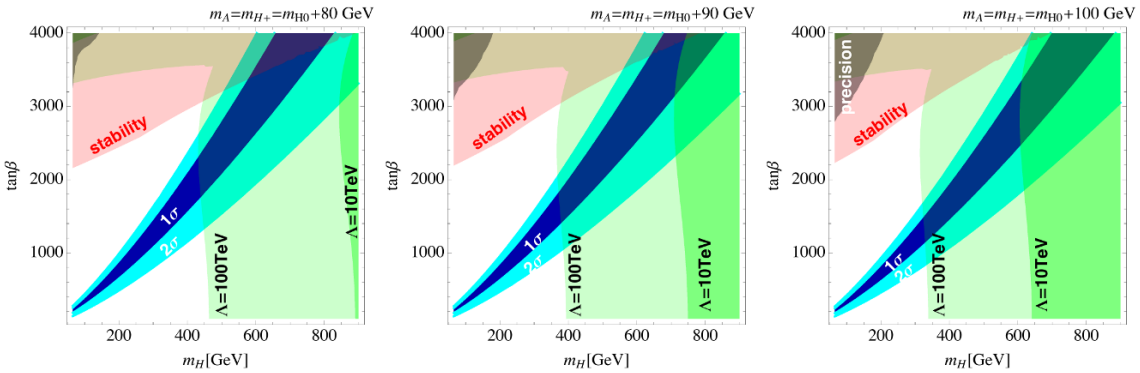

Figure 1. Regions where the prediction for the muon $g-2$ is consistent with the measurement within 1σ (blue) and 2σ (cyan). The green (darker green) region shows the cutoff scale to be less than 100 (10) TeV given by the perturbative unitarity bound (see section 3.2). The red region indicates the cutoff scale to be less than 10 TeV given by the vacuum stability bound (see section 3.2). The gray region is excluded by the electroweak precision measurements at 95% CL (see section 3.4).

enhanced by $\tan\beta$. As a result, these two-loop contributions can be comparable to the one-loop diagram. However, in the present model, the both tau and bottom Yukawa couplings are suppressed by $\cot\beta$ as seen in eq. (2.13). Therefore, the contribution from two-loop diagrams is simply suppressed by the loop factor, so that these cannot be important. We thus only consider the one-loop diagram for the muon $g-2$.

Numerical results for δa_μ are shown in figure 1 on the m_H–$\tan\beta$ plane. The blue and cyan regions show the regions of parameter space where we can explain the muon $g-2$ within 1σ and 2σ, respectively. Here, we consider the case with H^0 to be the lightest of all the additional Higgs bosons, and we display the three cases for the mass difference between m_H and $m_A(=m_{H^\pm})$ being 80 (left), 90 (center) and 100 (right) GeV. We can see that the prediction of δa_μ is not changed so much among these three cases. We find that the discrepancy of the muon $g-2$ becomes 1σ by taking, e.g., $m_H = 300(600)$ GeV with $\tan\beta = 1000\,(3000)$.

3.2 Constraints on scalar quartic couplings

The scalar quartic couplings λ_1–λ_5 in the Higgs potential can be constrained by taking into account the following theoretical arguments. Such constraint can be translated into the bound on the physical Higgs boson masses and mixing angles via eqs. (2.16)–(2.20).

First, the Higgs potential must be bounded from below in any direction of the scalar field space. The sufficient condition to guarantee the vacuum stability is given by [24–28]

$$\lambda_1 > 0, \quad \lambda_2 > 0, \quad \sqrt{\lambda_1\lambda_2} + \lambda_3 + \mathrm{MIN}(0, \lambda_4+\lambda_5, \lambda_4-\lambda_5) > 0. \tag{3.10}$$

Next, perturbative unitarity requires that s-wave amplitude matrices for elastic scatterings of scalar boson 2-body to 2-body processes must not be too large to satisfy S matrix unitarity. This perturbative unitarity condition is expressed as

$$|a^0_{i,\pm}| \leq \frac{1}{2}, \tag{3.11}$$

JHEP07(2017)012

where $a^0_{i,\pm}$ are the eigenvalues of such s-wave amplitude matrices. In the CP-conserving THDMs, these eigenvalues are given by [29–32]:

$$a^0_{1,\pm} = \frac{1}{32\pi}\left[3(\lambda_1+\lambda_2) \pm \sqrt{9(\lambda_1-\lambda_2)^2+4(2\lambda_3+\lambda_4)^2}\right], \tag{3.12}$$

$$a^0_{2,\pm} = \frac{1}{32\pi}\left[(\lambda_1+\lambda_2) \pm \sqrt{(\lambda_1-\lambda_2)^2+4\lambda_4^2}\right], \tag{3.13}$$

$$a^0_{3,\pm} = \frac{1}{32\pi}\left[(\lambda_1+\lambda_2) \pm \sqrt{(\lambda_1-\lambda_2)^2+4\lambda_5^2}\right], \tag{3.14}$$

$$a^0_{4,\pm} = \frac{1}{16\pi}(\lambda_3+2\lambda_4 \pm \lambda_5), \tag{3.15}$$

$$a^0_{5,\pm} = \frac{1}{16\pi}(\lambda_3 \pm \lambda_4), \tag{3.16}$$

$$a^0_{6,\pm} = \frac{1}{16\pi}(\lambda_3 \pm \lambda_5). \tag{3.17}$$

We impose the above two conditions given in eqs. (3.10) and (3.11) at an arbitrary energy scale μ. In this case, all the scalar quartic couplings λ_1–λ_5 should be understood as a function of μ, where their energy dependence are determined by solving renormalization group equations. In addition, we require that no Landau pole appears up to a certain energy scale, and we call this the triviality bound. From the above consideration, we can define the cutoff scale of the theory $\Lambda_{\rm cutoff}$ in such a way that one of the three conditions, i.e., the perturbative unitarity, the vacuum stability and the triviality bounds is not satisfied. The renormalization group equations are expressed by a set of β-functions for dimensionless parameters defined by

$$\mu\frac{d}{d\mu}c = \frac{1}{(4\pi)^2}\beta_c. \tag{3.18}$$

We calculate the β-functions by using `SARAH` [33]. They are approximately given as follows:

$$\beta_{g_1} \simeq 7g_1^3, \tag{3.19}$$

$$\beta_{g_2} \simeq -3g_2^3, \tag{3.20}$$

$$\beta_{g_3} \simeq -7g_3^3, \tag{3.21}$$

$$\begin{aligned}\beta_{\lambda_1} \simeq {}& +\frac{3}{4}g_1^4+\frac{3}{2}g_1^2g_2^2+\frac{9}{4}g_2^4-3g_1^2\lambda_1-9g_2^2\lambda_1+12\lambda_1^2+4\lambda_3^2+4\lambda_3\lambda_4+2\lambda_4^2+2\lambda_5^2\\ &+4\lambda_1y_\mu^2-4y_\mu^4,\end{aligned} \tag{3.22}$$

$$\begin{aligned}\beta_{\lambda_2} \simeq {}& +\frac{3}{4}g_1^4+\frac{3}{2}g_1^2g_2^2+\frac{9}{4}g_2^4-3g_1^2\lambda_2-9g_2^2\lambda_2+12\lambda_2^2+4\lambda_3^2+4\lambda_3\lambda_4+2\lambda_4^2+2\lambda_5^2\\ &+12\lambda_2y_t^2-12y_t^4,\end{aligned} \tag{3.23}$$

$$\begin{aligned}\beta_{\lambda_3} \simeq {}& \lambda_3\left(2y_\mu^2+6y_t^2-3g_1^2-9g_2^2+6\lambda_1+6\lambda_2+4\lambda_3\right)\\ &+\frac{3}{4}g_1^4-\frac{3}{2}g_1^2g_2^2+\frac{9}{4}g_2^4+2\lambda_1\lambda_4+2\lambda_2\lambda_4+2\lambda_4^2+2\lambda_5^2,\end{aligned} \tag{3.24}$$

$$\beta_{\lambda_4} \simeq 3g_1^2g_2^2+8\lambda_5^2+\lambda_4\left(2\lambda_1+2\lambda_2+8\lambda_3+4\lambda_4-3g_1^2-9g_2^2+2y_\mu^2+6y_t^2\right), \tag{3.25}$$

$$\beta_{\lambda_5} \simeq \lambda_5\left(2\lambda_1+2\lambda_2+8\lambda_3+12\lambda_4-3g_1^2-9g_2^2+2y_\mu^2+6y_t^2\right), \tag{3.26}$$

$$\beta_{y_t} \simeq \frac{9}{2}y_t^3+y_t\left(-8g_3^2-\frac{17}{12}g_1^2-\frac{9}{4}g_2^2\right), \tag{3.27}$$

$$\beta_{y_\mu} \simeq \frac{5}{2}y_\mu^3-\frac{3}{4}y_\mu\left(5g_1^2+3g_2^2\right). \tag{3.28}$$

JHEP07(2017)012

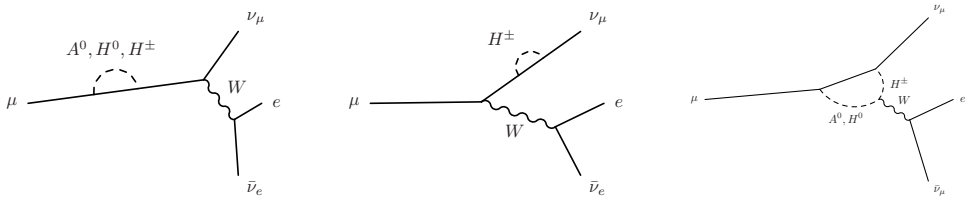

Figure 2. Leading diagrams for the one-loop correction to the muon decay.

Here, we take into account the y_t and y_μ dependence, and all the other Yukawa couplings are neglected because of their smallness. In addition, we ignore higher loop contributions.

In figure 1, we show the $\Lambda_{\rm cutoff}$ dependence on the m_H–$\tan\beta$ plane. The regions filled by green (darker green) indicate those with $\Lambda_{\rm cutoff} \leq 100$ (10) TeV due to the perturbative unitarity bound or the triviality bound. In addition, the regions filled by red show those with $\Lambda_{\rm cutoff} \leq 10\,\text{TeV}$ due to the vacuum stability condition. If we assume that the model is valid up to 10 TeV and explains the muon $g-2$ within 1σ, then the mass of H^0 should be smaller than 800 GeV.

3.3 Constraints from lepton flavor universality

As we discussed in section 2.2 and section 3.1, the muon Yukawa coupling can be order 1 in the large $\tan\beta$ scenario which is favored to explain the muon $g-2$ anomaly. Thanks to the muon-specific feature of this model, the tree level contribution of the charged Higgs exchanging diagram to the leptonic τ decay process is negligible because of the cancellation of the $\tan\beta$ dependence. This is the big difference in this model from the Type-X THDM. However, the large muon Yukawa coupling can break the lepton universality via the extra Higgs boson loop effects shown in figure 2. Thus, in this subsection, we study the constrains from the lepton universality at the one-loop level.

The modification of the W-μ-ν_μ coupling is expressed follows:

$$g_{W\mu\nu} \to g_{W\mu\nu}\,(1+\delta g)\,, \tag{3.29}$$

where

$$\delta g = \frac{1}{(4\pi)^2}\frac{m_\mu^2}{v^2}\tan^2\beta\left(1+\frac{m_{H^\pm}^2+m_A^2}{4(m_{H^\pm}^2-m_A^2)}\ln\frac{m_A^2}{m_{H^\pm}^2}+\frac{m_{H^\pm}^2+m_{H^0}^2}{4(m_{H^\pm}^2-m_{H^0}^2)}\ln\frac{m_{H^0}^2}{m_{H^\pm}^2}\right). \tag{3.30}$$

The other lepton couplings to the W boson ($g_{We\nu}$ and $g_{W\tau\nu}$) does not recieve loop corrections proportional to $\tan^2\beta$. In the case of $m_A = m_{H^\pm}$ which was taken in the calculation given in section 3.1, we obtain

$$\begin{aligned}\delta g &= \frac{1}{(4\pi)^2}\frac{m_\mu^2}{v^2}\tan^2\beta\left(\frac{1}{2}+\frac{m_{H^\pm}^2+m_H^2}{4(m_{H^\pm}^2-m_H^2)}\ln\frac{m_H^2}{m_{H^\pm}^2}\right)\\ &\simeq -3\times10^{-6}\left(\frac{\tan\beta}{1000}\right)^2\left(\frac{\Delta m}{80\,\text{GeV}}\right)^2\left(\frac{600\,\text{GeV}}{m_H}\right)^2,\end{aligned} \tag{3.31}$$

JHEP07(2017)012

where $\Delta m = m_{H^\pm} - m_H$. Since G_F is determined from the muon decay, this modification affects to the relations between G_F and v,

$$G_F \equiv \frac{1}{\sqrt{2}v^2}(1+\delta g)^2. \tag{3.32}$$

In order to check the lepton universality in terms of G_F calculated in eq. (3.32), we introduce the following quantities:

$$\left(\frac{G_{ba}}{G_F}\right)^2 \equiv \frac{\Gamma(a \to b\nu_a\bar{\nu}_b)}{\Gamma(\mu \to e\nu_\mu\bar{\nu}_e)} \tag{3.33}$$

The measured values by HFAG are [34]

$$\frac{G_{\mu\tau}}{G_{e\mu}} = 1.0029 \pm 0.0015, \quad \frac{G_{\mu\tau}}{G_{e\tau}} = 1.0018 \pm 0.0014. \tag{3.34}$$

The model prediction at the one-loop level is

$$\frac{G_{\mu\tau}}{G_{e\mu}} = 1, \quad \frac{G_{\mu\tau}}{G_{e\tau}} = (1+\delta g) \simeq 1 + \mathcal{O}(10^{-6}). \tag{3.35}$$

Therefore, we can safely avoid the constraint from the lepton universality even in the large $\tan\beta$ scenario.

3.4 Constraints from the electroweak precision measurements

The oblique S, T and U parameters introduced by Peskin and Takeuchi [35, 36] provide a convenient formalism to discuss the constraint on model parameters from electroweak precision measurements. However, we cannot simply apply this formalism to our model, because those parameters are formulated under the assumption that new particles do not give sizable direct corrections to light fermion (including the muon) scattering processes $f_1\bar{f}_2 \to f_3\bar{f}_4$ through vertex corrections and wave function renormalizations. The other assumption is that the new physics scale is sufficiently higher than the electroweak scale. In our setup, both of them cannot be justified. Hence we need to modify the formulation with the S, T and U parameters by taking into account vertex corrections and wave function renormalizations.

By varying the four model parameters (m_H, m_A, $m_{H^\pm}$, t_β), we find that the minimum value of χ^2 to be $\chi^2_{\text{min.}} = 23.7587$ which is given at (m_H, m_A, $m_{H^\pm}$, t_β) = (59.4 GeV, 398 GeV, 402 GeV, 686). We calculate $\Delta\chi^2 \equiv \chi^2 - \chi^2_{\text{min.}}$ by varying m_H and t_β with fixed values for m_A and $m_{H^\pm}$. The result is shown in figure 1 where the gray region is excluded at 95% CL. The detail of our analysis is given in appendix C.

3.5 Constraints and signatures at the LHC experiment

Finally, we discuss the constraint on parameters from current LHC data.

In our model, the quark Yukawa couplings to the additional Higgs bosons are highly suppressed by $\cot\beta$ in the large $\tan\beta$ regime. Therefore, the additional neutral Higgs bosons A^0 and H^0 cannot be produced via the gluon fusion process: $gg \to A^0/H^0$. For the

JHEP07(2017)012

m_{H^0} [GeV]	$m_{A^0}(=m_{H^\pm})$ [GeV]	$\tan\beta$	$\sigma_{13\text{TeV}}$ [fb]	$N_{\mu\text{-THDM}}$	$\mathcal{L}_{3\sigma}$ [fb^{-1}]
600	700	3000	0.41	6.6	–
620	710	3000	0.369	5.9	–
640	730	3100	0.316	5.2	44
660	750	3300	0.2707	4.5	58
680	770	3400	0.2334	3.9	75
700	790	3700	0.20	3.4	97

Table 2. The parameter points that we investigate. $\sigma_{13\text{TeV}}$ is defined in eq. (3.40). $N_{\mu\text{-THDM}}$ is the expected signal event numbers in the last bin of figure 2(b) in ref. [40]. $\mathcal{L}_{3\sigma}$ is the integrated luminosity at which we can expect 3σ deviation from the SM prediction if we apply the same analysis as ref. [40]. The data points with "-" in the last column are already excluded.

same reason, the $gb \to tH^-$ process for the $H^\pm$ production also does not work. Moreover, the vector boson fusion process: $qQ \to q'Q'H^0$ is negligible, because the H^0VV couplings are proportional to $c_{\beta-\alpha}$. As a result, the main production mode for these Higgs bosons is their pair productions via the s-channel mediation of a virtual gauge boson:

$$pp \to Z^* \to H^0A^0, \quad pp \to W^* \to H^\pm A^0/H^\pm H^0, \quad pp \to \gamma^*/Z^* \to H^+H^-. \tag{3.36}$$

Because of the muon specific property, the decay branching ratios for H^0, A^0, and $H^\pm$ with the parameter choice in figure 1 are given as follows:

$$\text{Br}(H^0 \to \mu\bar{\mu}) \simeq 1, \tag{3.37}$$

$$\text{Br}(A^0 \to \mu\bar{\mu}) + \text{Br}(A^0 \to H^0Z) \simeq 1, \tag{3.38}$$

$$\text{Br}(H^- \to \mu\bar{\nu}_\mu) + \text{Br}(H^- \to H^0W^-) \simeq 1. \tag{3.39}$$

The relative magnitude between the above two branching ratios of A^0 and that of $H^\pm$ mainly depends on the values of t_β and the mass difference between m_H and $m_{H^\pm}$. For example, we obtain $\text{Br}(A^0 \to \mu\bar{\mu})$ and $\text{Br}(H^- \to \mu\bar{\nu}_\mu)$ to be about 89(99.1)% and 96(99.7)% for $m_H = 300(600)\,\text{GeV}$, $m_{H^\pm} - m_H = 100\,\text{GeV}$ and $t_\beta = 1000(3000)$, respectively. Therefore, the collider signature of the model is multi-muon final states.

We show the production cross sections in some parameter points given in table 2. Here, the production cross section is defined as the sum of all the modes given in eq. (3.36) at 13 TeV,

$$\sigma_{13\text{TeV}} \equiv \sum_{X=A^0,H^\pm} \sigma(pp \to H^0X) + \sum_{Y=H^\pm} \sigma(pp \to A^0Y) + \sigma(pp \to H^+H^-). \tag{3.40}$$

We generate `UFO` files [37] by using `FeynRules 2.3.3` [38], and use `MadGraph 5` [39] to estimate the production cross sections. Signal events are simulated by using `MadGraph 5`, `PYTHIA 6.428` [41], and `DELPHES 3.3.3` [42]. We compare the number of events predicted in our model with that of the CMS result for the multi-lepton signal search at 13 TeV with 35.9 fb^{-1} data [40]. We find the last bin of figure 2(b) in ref. [40] gives the stringent bound on the mass of H^0 because our model predicts three-muon final states with large p_T, e.g., via $pp \to H^0H^\pm \to \mu^+\mu^-\mu^\pm\nu$. The observed (expected) background event number in the bin is 3(3.5). The expected signal event numbers in several parameter points are shown

JHEP07(2017)012

in table 2. We use the CLs method [43–45], and find that the region with $m_H \lesssim 640\,\text{GeV}$ is excluded at 95% CL. Also, we show the integrated luminosity which is required to give the 3σ deviation from the SM expectation for each parameter point. We can see that the allowed parameter points ($m_H \geq 640\,\text{GeV}$) could give the 3σ deviation during the LHC Run 2 experiment.

4 Conclusions

We have investigated a new type of the THDM, i.e. μTHDM, as a solution of the muon $g-2$ anomaly. Differently from the other THDMs with a softly-broken Z_2 symmetry, this model predicts that only the muon couplings to the additional Higgs bosons are enhanced by $\tan\beta$, while all the other SM fermion couplings to them are suppressed by $\cot\beta$. Thanks to this coupling property, the μTHDM can avoid the strong constraint from the leptonic τ decay in contrast to the Type-X THDM which cannot explain the muon $g-2$ within the 1σ level due to this constraint. We find that the μTHDM can explain the muon $g-2$ within the 1σ level satisfying constraints from perturbative unitarity, vacuum stability, electroweak precision measurements, and current LHC data.

We have found that large $\tan\beta$ is required to solve the muon $g-2$ anomaly within the 1σ level. Its typical values is $\mathcal{O}(1000)$ with the masses of the additional Higgs bosons to be in the range of 100–1000 GeV. The large $\tan\beta$ is equivalent to the large muon Yukawa coupling, $y_\mu \sim \mathcal{O}(1)$. In order to see the effect of such large Yukawa coupling, we have studied the constraints from the perturbative unitarity and the vacuum stability conditions. We have found that the smaller mass regime for the additional Higgs bosons is preferable. For example, if we require the cutoff scale of this model to be above 10 TeV, H^0 should be lighter than 800 GeV in the case of $m_A = m_{H^\pm} = m_H + 90\,\text{GeV}$ and $\sin(\beta-\alpha) = 1$. Another consequence of the large Yukawa coupling is multi-muon final states at the LHC. We have found that the region with $m_H \lesssim 640\,\text{GeV}$ is excluded at 95% CL by the LHC data with 13 TeV of the collision energy and $35.9\,\text{fb}^{-1}$ of the integrated luminosity. From these constraints, we conclude that the cutoff scale of the μTHDM is higher than 10 TeV but have to be lower than 100 TeV if the model solves the muon $g-2$ anomaly within 1σ level.

At the end, we briefly discuss how to weaken the constraint from the multi-muon signature at the LHC and make the cutoff scale higher. One possible way is to add neutral and stable particles which couple to the additional Higgs bosons. Then new decay modes of the additional Higgs bosons can open and the rate of the multi-muon final state can be reduced. Another way is to embed this model into the context of composite THDMs [46–48] whose typical cutoff scale is around 10 TeV. In that case, the model should be emerged from (unknown) UV dynamics.

Acknowledgments

We would like to thank Howard E. Haber and Pedro Ferreira for their comments. We also thank Mihoko M. Nojiri and Michihisa Takeuchi for their comments on LHC phenomenology. This work was supported by JSPS KAKENHI Grant Number 16K17715 [TA].

JHEP07(2017)012

A Neutrino mass and mixing

The observation of the neutrino oscillation shows three flavors of neutrinos ν_e, ν_μ, and ν_τ are mixed by large angles. However, the global symmetry in our setup might forbid the mixing ν_μ with the other neutrinos. In this section, we discuss dimension five operators for the Majorana neutrino mass matrices to see if they respect some symmetries.

The dimension five operators are given as follows.

$$-\frac{c_{11}^{ij}}{M_{11}}(\overline{(L_L^i)}\tilde{H}_1)(\widetilde{H}_1^T(L_L^c)^j) - \frac{c_{12}^{ij}}{M_{12}}(\overline{(L_L^i)}\tilde{H}_1)(\widetilde{H}_2^T(L_L^c)^j) \tag{A.1}$$

$$-\frac{c_{21}^{ij}}{M_{21}}(\overline{(L_L^i)}\tilde{H}_2)(\widetilde{H}_1^T(L_L^c)^j) - \frac{c_{22}^{ij}}{M_{22}}(\overline{(L_L^i)}\tilde{H}_2)(\widetilde{H}_2^T(L_L^c)^j) \tag{A.2}$$

$$+\,(\text{h.c.}). \tag{A.3}$$

The Z_4 symmetry restricts the structure of the coefficient matrices as follows.

$$c_{11} = \begin{pmatrix} (c_{11})^{ee} & (c_{11})^{e\tau} & 0 \\ (c_{11})^{\tau e} & (c_{11})^{\tau\tau} & 0 \\ 0 & 0 & 0 \end{pmatrix}, \quad c_{12} = \begin{pmatrix} 0 & 0 & 0 \\ 0 & 0 & 0 \\ 0 & 0 & (c_{12})^{\mu\mu} \end{pmatrix}, \tag{A.4}$$

$$c_{21} = \begin{pmatrix} 0 & 0 & 0 \\ 0 & 0 & 0 \\ 0 & 0 & (c_{21})^{\mu\mu} \end{pmatrix}, \qquad c_{22} = \begin{pmatrix} (c_{22})^{ee} & (c_{22})^{e\tau} & 0 \\ (c_{22})^{\tau e} & (c_{22})^{\tau\tau} & 0 \\ 0 & 0 & 0 \end{pmatrix}. \tag{A.5}$$

From these matrices, we obtain the block diagonalized neutrino mass matrix, and thus the PMNS matrix is also block diagonalized. This is inconsistent with the large mixing angle between ν_μ and $\nu_{e,\tau}$. To obtain a realistic neutrino mass matrix, we add an SU(2) triplet scalar with $Y = -1$ (Δ) which transforms under the Z_4 symmetry as $\Delta \to -i\Delta$. Using Δ, we obtain following terms,

$$-c_\Delta^{ij}\bar{L}_L^i\Delta(L_L^c)^j, \tag{A.6}$$

where

$$c_\Delta = \begin{pmatrix} 0 & 0 & (c_\Delta)^{e\mu} \\ 0 & 0 & (c_\Delta)^{\tau\mu} \\ (c_\Delta)^{\mu e} & (c_\Delta)^{\mu\tau} & 0 \end{pmatrix}. \tag{A.7}$$

Δ obtains its VEV because of the coupling with the Higgs field via the following softly Z_4 breaking interactions:

$$\mathcal{L} = \kappa_{11}\Delta H_1 H_1 + \kappa_{12}\Delta H_1 H_2 + \kappa_{22}\Delta H_2 H_2 + (\text{h.c.}). \tag{A.8}$$

Using eqs. (A.3), (A.7), and (A.8), we can obtain the neutrino mass matrix generated that does not contain zero-components,

$$m_\nu = \begin{pmatrix} (m_\nu)^{ee} & (m_\nu)^{e\tau} & (m_\nu)^{e\mu} \\ (m_\nu)^{\tau e} & (m_\nu)^{\tau\tau} & (m_\nu)^{\tau\mu} \\ (m_\nu)^{\mu e} & (m_\nu)^{\mu\tau} & (m_\nu)^{\mu\mu} \end{pmatrix}. \tag{A.9}$$

JHEP07(2017)012

	q_L^j	u_R^j	d_R^j	ℓ_L^e	ℓ_L^τ	ℓ_L^μ	e_R	τ_R	μ_R	H_1	H_2
$\mathrm{SU}(3)_c$	3	3	3	1	1	1	1	1	1	1	1
$\mathrm{SU}(2)_L$	2	1	1	2	2	2	1	1	1	2	2
$\mathrm{U}(1)_Y$	1/6	2/3	−1/3	−1/2	−1/2	−1/2	−1	−1	−1	1/2	1/2
Z_N	1	1	1	1	1	ω^a	1	1	ω^b	ω^c	1

Table 3. The matter contents and the charge assignments. Here $\omega = \exp(2\pi i/N)$.

It is possible to obtain realistic neutrino masses and the PMNS matrix from eq. (A.9) without hard breaking of Z_4 symmetry. We do not further discuss the neutrino physics in this paper. As long as all the particles that arise from Δ are much heavier than all the other particles, they are irrelevant with the phenomenology at the collider experiments. In this sense, an extension which is discussed here does not affect to our analysis in the main part of this paper.

B Other discrete symmetries for μTHDM

We briefly discuss other realizations of the μTHDM. We assume a Z_N symmetry to avoid FCNCs at the tree level. It might be possible to use the other discrete symmetries for the realization of the model, but it is beyond the scope here.

Similar to the Z_4 symmetry discussed in the main part of this paper, we assign non-trivial Z_N charges to ℓ_L^μ, μ_R, and H_1. All the other fields are singlet under the Z_N symmetry. The charge assignment is summarized in table 3, where a, b, and c are integers, $a, b, c = 0, 1, 2, \cdots N-1$. The Z_N charges have to satisfy the following conditions in order to obtain the muon specific texture for the lepton Yukawa matrices given in eq. (2.3).

$$a \neq 0, \qquad b \neq 0, \quad c \neq 0, \tag{B.1}$$

$$-a + c \neq 0, \quad b + c \neq 0, \tag{B.2}$$

$$-a + b + c = 0. \tag{B.3}$$

These conditions requires $N \geq 3$.

The Z_N symmetry with the above conditions forbids $(H_1^\dagger H_1)(H_1^\dagger H_2)$ and $(H_2^\dagger H_2)(H_2^\dagger H_1)$. Therefore the Higgs potential is given by eq. (2.4). The Z_N symmetry can also forbid the λ_5 term in the Higgs potential, $(H_1^\dagger H_2)^2$, if $\omega^{2c} \neq 1$.

Let us here discuss what happens if $\lambda_5 = 0$. In this case, the masses of H^0 and A^0 are degenerate in the large $\tan\beta$ limit. This can be understood by noting the appearance of an accidental global U(1) symmetry in the Higgs potential, which is similar to the Peccei-Quinn symmetry. Namely, the absence of the λ_5 and m_3^2 terms, the latter happens due to the large $\tan\beta$ limit under a fixed value of M^2 (see eq. (2.10)), makes the Higgs potential invariant under the transformation, $H_{1,2} \to \exp(i\theta_{1,2})H_{1,2}$. This symmetry forces the CP-even neutral scalar to have the degenerate mass with the CP-odd neutral scalar.

This mass degeneracy reduces the contribution to the muon $g-2$, because the A^0 and H^0 loop effects are destructive. In order to compensate this reduction, we need to

take smaller masses of A^0 and H^0. However, smaller masses are highly disfavored by the searches of multi-lepton final state at the LHC as discussed in section 3.5. This is the reason why we choose the case with $\lambda_5 \neq 0$ which is realized by $\omega^{2c} = 1$ as mentioned above, and the Z_4 symmetry corresponds to the minimal choice for the realization of non-zero λ_5.

C Details on the constraints from the electroweak precision measurements

We choose $\alpha_{\rm em}$, m_Z, and $\sqrt{2}G_F$ as the input parameters. They relate to the model parameters as follows.

$$4\pi\alpha_{\rm em} = \frac{1}{1 - \frac{d\Pi_{\gamma\gamma}}{dq^2}(m_Z^2)} \left(\frac{1}{g^2} + \frac{1}{g'^2}\right)^{-2}, \tag{C.1}$$

$$m_Z^2 = \frac{g^2 + g'^2}{4} v^2 + \Pi_{ZZ}(m_Z^2), \tag{C.2}$$

$$\sqrt{2}G_F = \frac{1}{v^2}\left(1 + \frac{\delta g_W^\mu}{g} - \frac{\Pi_{WW}(0)}{\frac{g^2}{4}v^2}\right), \tag{C.3}$$

where $v^2 = v_1^2 + v_2^2$, g is the $\mathrm{SU}(2)_L$ gauge coupling, g' is the $\mathrm{U}(1)_Y$ gauge coupling, Π_{ij}'s are the gauge boson self-energies, and δg_W^μ is the sum of the vertex corrections to W-μ-ν_μ coupling at zero momentum with the wave function renormalization effects. The Fermi constant receives the non-negligible effect from the vertex correction as can be seen eq. (C.3). Therefore the vertex correction δg_W^μ affects every observables through the replacement of v^2 by G_F. This effect is a reason why we cannot use the S, T and U parameters directly.

We derive the deviations of the model prediction from the SM prediction in the same manner as in [35, 36], $\Delta O \equiv \mathcal{O}_{\rm model} - \mathcal{O}_{\rm SM}$. The result is complicated but summarized by the following modified version of the S, T and U parameters.

$$\alpha_{\rm em}\tilde{T} = \left(\frac{\Pi_{WW}(0)}{m_W^2} - \frac{\delta g_W^\mu}{g}\right) - \frac{\Pi_{ZZ}(0)}{m_Z^2}, \tag{C.4}$$

$$\frac{\alpha_{\rm em}}{4s_0^2c_0^2}\tilde{S} = \frac{\Pi_{ZZ}(m_Z^2) - \Pi_{ZZ}(0)}{m_Z^2} - \frac{c_0^2 - s_0^2}{c_0 s_0}\frac{\Pi_{Z\gamma}(m_Z^2)}{m_Z^2} - \frac{\Pi_{\gamma\gamma}(m_Z^2)}{m_Z^2}, \tag{C.5}$$

$$\frac{\alpha_{\rm em}}{4s_0^2}(\tilde{S} + \tilde{U}) = \frac{\Pi_{WW}(m_W^2) - \Pi_{WW}(0)}{m_W^2} + \frac{\delta g_W^\mu}{g} - \frac{c_0}{s_0}\frac{\Pi_{Z\gamma}(m_Z^2)}{m_Z^2} - \frac{\Pi_{\gamma\gamma}(m_Z^2)}{m_Z^2}, \tag{C.6}$$

$$\alpha_{\rm em}\tilde{W} = \frac{d\Pi_{WW}}{dq^2}(m_W^2) - \frac{\Pi_{WW}(m_W^2) - \Pi_{WW}(0)}{m_W^2} - \frac{\delta g_W^\mu}{g_W}, \tag{C.7}$$

$$\alpha_{\rm em}\tilde{Z} = \frac{d\Pi_{ZZ}}{dq^2}(m_Z^2) - \frac{\Pi_{ZZ}(m_Z^2) - \Pi_{ZZ}(0)}{m_Z^2}. \tag{C.8}$$

We also use s_0^2 and $c_0^2 = 1 - s_0^2$ that are defined by the input values as

$$s_0^2 c_0^2 = \frac{\alpha_{\rm em}\pi}{m_Z^2\sqrt{2}G_F}. \tag{C.9}$$

JHEP07(2017)012

$\tilde{S}$ is the same as S defined in PDG [49]. If $\delta g_W^\mu/g = 0$, then, $\tilde{T}$ and $\tilde{U}$ becomes the same as T and U given in PDG, respectively. $\tilde{W}$ and $\tilde{Z}$ are negligible if new particles are much heavier than the electroweak gauge bosons. They cannot be ignored in our setup. In $\delta g_W^\mu/g \to 0$ limit, $\tilde{W}$ and $\tilde{Z}$ becomes W and V defined in [50, 51], respectively. Using these parameters, we find the following expressions for $\Delta O \equiv \mathcal{O}_{\rm model} - \mathcal{O}_{\rm SM}$.

$$\Delta m_W = \frac{1}{4}\frac{1}{s_0}\left(\frac{4\pi\alpha_{\rm em}}{\sqrt{2}G_F}\right)^{1/2}\left[-\frac{\alpha_{\rm em}}{2(c_0^2-s_0^2)}\tilde{S} + \frac{c_0^2}{c_0^2-s_0^2}\alpha_{\rm em}\tilde{T} + \frac{\alpha_{\rm em}}{4s_0^2}\tilde{U}\right], \tag{C.10}$$

$$\Delta\Gamma(W\to ff') = \frac{m_W N_c}{12}\frac{\alpha_{\rm em}}{s_0^2}\left[-\frac{1}{2(c_0^2-s_0^2)}\alpha_{\rm em}\tilde{S} + \frac{c_0^2}{c_0^2-s_0^2}\alpha_{\rm em}\tilde{T} + \frac{\alpha_{\rm em}}{4s_0^2}\tilde{U} + \alpha_{\rm em}\tilde{W} + 2\frac{\delta g_{Wff'}(m_W)}{g_W}\right], \tag{C.11}$$

$$\begin{aligned}\Delta\Gamma(Z\to ff') = \frac{m_Z}{24}N_c\Bigg[&-Q(j_3-2s_0^2Q)\frac{\alpha_{\rm em}\tilde{S}}{2(c_0^2-s_0^2)} \\ &+\left(\left((j_3-s_0^2Q)^2+(-s_0^2Q)^2\right)+2Q(j_3-2s_0^2Q)\frac{s_0^2c_0^2}{c_0^2-s_0^2}\right)\alpha_{\rm em}\tilde{T} \\ &+\left((j_3-s_0^2Q)^2+(-s_0^2Q)^2\right)\alpha_{\rm em}\tilde{Z} \\ &+2(j_3-s_0^2Q)\left(\frac{\delta g^L_{Zff'}}{g_Z}\right)-2s_0^2Q\left(\frac{\delta g^R_{Zff'}}{g_Z}\right)\Bigg],\end{aligned} \tag{C.12}$$

$$\Delta A_f = \frac{4s_0^2Q(j_3-s_0^2Q)}{[(j_3-s_0^2Q)^2+(s_0^2Q)^2]^2}\left[-j_3Q\frac{\alpha_{\rm em}\tilde{S}}{4(c_0^2-s_0^2)} + j_3Q\frac{s_0^2c_0^2}{c_0^2-s_0^2}\alpha_{\rm em}\tilde{T} + \frac{\delta g^L_{Zff'}}{g_Z} + \frac{\delta g^R_{Zff'}}{g_Z}\right], \tag{C.13}$$

$$\Delta A_{FB}^{0,f} = \frac{3}{4}\left(\Delta A_f A_e^{\rm SM} + A_f^{\rm SM}\Delta A_e\right), \tag{C.14}$$

$$\Delta R_\ell \simeq R_\ell^{\rm SM}\left(\frac{\Delta\Gamma(Z\to had)}{\Gamma(Z\to had)\,|_{\rm SM}} - \frac{\Delta\Gamma(Z\to \ell\ell)}{\Gamma(Z\to \ell\ell)\,|_{\rm SM}}\right), \tag{C.15}$$

$$\Delta R_q \simeq R_q^{\rm SM}\left(\frac{\Delta\Gamma(Z\to qq)}{\Gamma(Z\to qq)\,|_{\rm SM}} - \frac{\Delta\Gamma(Z\to had)}{\Gamma(Z\to had)\,|_{\rm SM}}\right), \tag{C.16}$$

where j_3 and Q are isospin and electric charge of external fermions, resepctively. $N_c = 3$ (for external quarks) or 1 (for external leptons). We also introduced the following quantities:

$$g_W = \left(\frac{4\pi\alpha_{\rm em}}{s_0^2}\right)^{1/2}, \tag{C.17}$$

$$g_Z = \left(\frac{4\pi\alpha_{\rm em}}{s_0^2c_0^2}\right)^{1/2}, \tag{C.18}$$

$$\Gamma(Z\to had) = \sum_q \Gamma(Z\to qq), \tag{C.19}$$

and $\delta g^{L,R}_{Zff'}$ are calculated at $q^2 = m_Z^2$. $\delta g_{Wff'}(m_W)$ and $\delta g^{L,R}_{Zff'}$ are only relevant for the muon sector and negligible in the other sector.

JHEP07(2017)012

Quantity	Value	SM
m_W[GeV]	80.385 ± 0.015	80.361 ± 0.006
Γ_W[GeV]	2.085 ± 0.042	2.089 ± 0.001
Γ_Z[GeV]	2.4952 ± 0.0023	2.4943 ± 0.0008
Γ(had)[GeV]	1.7444 ± 0.0020	1.7420 ± 0.0008
Γ(inv)[MeV]	499.0 ± 1.5	501.66 ± 0.05
$\Gamma(\ell^+\ell^-)$[MeV]	83.984 ± 0.086	83.995 ± 0.010
$\Gamma(\mu\mu)$[MeV]	83.99 ± 0.18	83.995 ± 0.010
R_e	20.804 ± 0.050	20.734 ± 0.010
R_μ	20.785 ± 0.033	20.734 ± 0.010
R_τ	20.764 ± 0.045	20.779 ± 0.010
R_b	0.21629 ± 0.00066	0.21579 ± 0.00003
R_c	0.1721 ± 0.0030	0.17221 ± 0.00003
$A_{FB}^{(0,e)}$	0.0145 ± 0.0025	0.01622 ± 0.00009
$A_{FB}^{(0,\mu)}$	0.0169 ± 0.0013	0.01622 ± 0.00009
$A_{FB}^{(0,\tau)}$	0.0188 ± 0.0017	0.01622 ± 0.00009
$A_{FB}^{(0,b)}$	0.0992 ± 0.0016	0.1031 ± 0.0003
$A_{FB}^{(0,c)}$	0.0707 ± 0.0035	0.0736 ± 0.0002
$A_{FB}^{(0,s)}$	0.0876 ± 0.0114	0.1032 ± 0.0003
A_e	0.1515 ± 0.0019	0.1470 ± 0.0004
A_μ	0.142 ± 0.015	0.1470 ± 0.0004
A_τ	0.143 ± 0.004	0.1470 ± 0.0004
A_b	0.923 ± 0.020	0.9347
A_c	0.670 ± 0.027	0.6678 ± 0.0002
A_s	0.90 ± 0.09	0.9356

Table 4. The electroweak precision data given by PDG [49].

We use the values given by PDG [49]. Input parameters are

$$G_F = 1.166378710^{-5}\ \text{GeV}^{-2}, \quad m_Z = 91.1876\ \text{GeV}, \quad \alpha_{\text{em}}^{-1}(m_Z) = 127.950, \tag{C.20}$$

$$m_\mu = 0.1056583745\ \text{GeV}, \tag{C.21}$$

The SM predictions and the values to be fitted are given in table 4. We construct likelihood function,

$$\chi^2 = \sum_O \left(\frac{\Delta O - (O_{\text{obs}} - O_{\text{SM}})}{\sigma_{\text{obs}}} \right)^2, \tag{C.22}$$

and perform the χ^2 analysis.

JHEP07(2017)012

We apply the above formula to the μTHDM. For $\sin(\beta-\alpha)=1$, we find

$$\Pi_{WW}(p^2) = -\frac{g_W^2}{4(4\pi)^2}\Big[A_0(m_A^2)+A_0(m_H^2)+2A_0(m_{H^\pm}^2) - 4B_{00}(p^2,m_H^2,m_{H^\pm}^2)-4B_{00}(p^2,m_A^2,m_{H^\pm}^2)\Big], \tag{C.23}$$

$$\Pi_{ZZ}(p^2) = -\frac{g_Z^2}{4(4\pi)^2}\Bigg[A_0(m_A^2)+A_0(m_H^2)+2(c_0^2-s_0^2)^2A_0(m_{H^\pm}^2) - 4B_{00}(p^2,m_H^2,m_A^2)-4(c_0^2-s_0^2)^2B_{00}(p^2,m_{H^\pm}^2,m_{H^\pm}^2)\Bigg], \tag{C.24}$$

$$\Pi_{\gamma\gamma}(p^2) = \frac{e^2}{(4\pi)^2}\Big[-2A_0(m_{H^\pm}^2)+4B_{00}(p^2,m_{H^\pm}^2,m_{H^\pm}^2)\Big], \tag{C.25}$$

$$\Pi_{Z\gamma}(p^2) = \frac{c_0^2-s_0^2}{2s_0c_0}\Pi_{\gamma\gamma}(p^2), \tag{C.26}$$

$$\begin{aligned}\delta g^L_{Z\mu\mu} \simeq{}& \frac{g_Z}{(4\pi)^2}\frac{m_\mu^2}{v^2}\tan^2\beta \\ &\times\Bigg(-\frac{1}{2}\Big[B_{1(\mu,\mu,a)}+B_{1(\mu,\mu,H)}+4C_{00(Z,\mu,\mu,H,A,\mu)}\Big] \\ &\quad+s_0^2\Big[-1+B_{1(\mu,\mu,A)}+B_{1(\mu,\mu,H)}+2C_{00(Z,\mu,\mu,\mu,\mu,A)}+2C_{00(Z,\mu,\mu,\mu,\mu,H)} \\ &\qquad-m_Z^2C_{12(\mu,Z,\mu,A,\mu,\mu)}-m_Z^2C_{12(\mu,Z,\mu,H,\mu,\mu)}\Big]\Bigg),\end{aligned} \tag{C.27}$$

$$\begin{aligned}\delta g^R_{Z\mu\mu} \simeq{}& \frac{g_Z}{(4\pi)^2}\frac{m_\mu^2}{v^2}\tan^2\beta \\ &\times\Bigg(-C_{00(Z,\mu,\mu,\mu,\mu,A)}-C_{00(Z,\mu,\mu,\mu,\mu,H)}+2C_{00(Z,\mu,\mu,0,0,H^\pm)} \\ &\quad+2C_{00(Z,\mu,\mu,H,A,\mu)}-2C_{00(Z,\mu,\mu,H^\pm,H^\pm,0)} \\ &\quad+\frac{1}{2}m_Z^2\left[C_{12(\mu,Z,\mu,A,\mu,\mu)}+C_{12(\mu,Z,\mu,H,\mu,\mu)}-2C_{12(\mu,Z,\mu,H^\pm,0,0)}\right] \\ &\quad+s_0^2\Bigg[-1+B_{1(\mu,\mu,A^0)}+B_{1(\mu,\mu,H)}+2C_{00(Z,\mu,\mu,\mu,\mu,A)}+2C_{00(Z,\mu,\mu,\mu,\mu,H)} \\ &\qquad+2B_{1(\mu,0,H^\pm)}+4C_{00(Z,\mu,\mu,H^\pm,H^\pm,0)} \\ &\qquad-m_Z^2C_{12(\mu,Z,\mu,A,\mu,\mu)}-m_Z^2C_{12(\mu,Z,\mu,H,\mu,\mu)}\Bigg]\Bigg),\end{aligned} \tag{C.28}$$

$$\begin{aligned}\delta g^L_{Z\nu_\mu\nu_\mu} \simeq{}& \frac{g_Z}{(4\pi)^2}\frac{m_\mu^2}{v^2}\tan^2\beta \\ &\times\Bigg(B_{1(0,\mu,H^\pm)}+2C_{00(Z,0,0,H^\pm,H^\pm,\mu)} \\ &+s_0^2\Big[4C_{00(0,Z,0,H^\pm,\mu,\mu)}-4C_{00(Z,0,0,H^\pm,H^\pm,\mu)}-2m_Z^2C_{12(0,Z,0,H^\pm,\mu,\mu)}-1\Big]\Bigg),\end{aligned} \tag{C.29}$$

JHEP07(2017)012

$$\delta g^L_{W\mu\nu_\mu}(m_W^2) \simeq \frac{g_W}{(4\pi)^2}\frac{m_\mu^2}{v^2}\tan^2\beta \times\left(-\frac{1}{2}-\frac{1}{4}B_0(_{0,A,A})-\frac{1}{4}B_0(_{0,H,H})-\frac{1}{2}B_0(_{0,H^\pm,H^\pm}) + 2C_{00}(_{0,W,0,0,A,H^\pm})+2C_{00}(_{0,W,0,0,H,H^\pm})\right), \tag{C.30}$$

$$\delta g^\mu_W \simeq \frac{g_W}{(4\pi)^2}\frac{m_\mu^2}{v^2}\tan^2\beta\left(1-\frac{m_A^2+m_{H^\pm}^2}{4(m_A^2-m_{H^\pm}^2)}\ln\frac{m_A^2}{m_{H^\pm}^2}-\frac{m_H^2+m_{H^\pm}^2}{4(m_H^2-m_{H^\pm}^2)}\ln\frac{m_H^2}{m_{H^\pm}^2}\right). \tag{C.31}$$

where

$$(_{a,b,c,\cdots}) = (m_a^2, m_b^2, m_c^2, \cdots), \tag{C.32}$$

$$(_{\cdots,0,\cdots}) = (\cdots, 0, \cdots). \tag{C.33}$$

The notation of A, B, and C function is the same as the notation used by `LoopTools` [52].

$$A_0(m^2) = m^2\left(\frac{1}{\bar\epsilon}+1+\ln\frac{\mu^2}{m^2}\right), \tag{C.34}$$

$$B_0(q^2,m_1^2,m_2^2) = \frac{1}{\bar\epsilon}+\int_0^1 dx\ln\frac{\mu^2}{m_1^2x+m_2^2(1-x)-q^2x(1-x)}, \tag{C.35}$$

$$B_1(q^2,m_1^2,m_2^2) = -\frac{1}{2\bar\epsilon}-\int_0^1 dx(1-x)\ln\frac{\mu^2}{m_1^2x+m_2^2(1-x)-q^2x(1-x)}, \tag{C.36}$$

$$B_{00}(q^2,m_1^2,m_2^2) = \frac{1}{4}\left(\frac{1}{\bar\epsilon}+1\right)\left[m_1^2+m_2^2-\frac{1}{3}q^2\right] + \frac{1}{2}\int_0^1 dx(m_1^2x+m_2^2(1-x)-q^2x(1-x)) \times\ln\frac{\mu^2}{m_1^2x+m_2^2(1-x)-q^2x(1-x)}, \tag{C.37}$$

$$C_{00}(p_1^2,p_2^2,p_3^2,m_1^2,m_2^2,m_3^2) = \frac{1}{4\bar\epsilon}+\frac{1}{2}\int_{xyz}\ln\frac{\mu^2}{m_1^2x+m_2^2y+m_3^2z-p_1^2xy-p_2^2yz-p_3^2zx}, \tag{C.38}$$

$$C_{12}(p_1^2,p_2^2,p_3^2,m_1^2,m_2^2,m_3^2) = -\int_{xyz}\frac{yz}{m_1^2x+m_2^2y+m_3^2z-p_1^2xy-p_2^2yz-p_3^2zx}. \tag{C.39}$$

where

$$\int_{xyz} = \int dxdydz\delta(x+y+z-1) = \int_0^1 dx\int_0^{1-x}dy \tag{C.40}$$

We vary the four model parameters (m_H, m_A, $m_{H^\pm}$, t_β) and try to fit the 24 observables in table 4. We find that the minimum value of χ^2 is given by $\chi^2_{\text{min.}} = 23.7587$ at (m_H, m_A, $m_{H^\pm}$, t_β) = (59.4 GeV, 398 GeV, 402 GeV, 686). We calculate $\Delta\chi^2 \equiv \chi^2 - \chi^2_{\text{min.}}$ by varying m_H and t_β with fixed values for m_A and $m_{H^\pm}$. The result is shown in figure 1 where the gray region is excluded at 95% CL.

JHEP07(2017)012

References

[1] Muon $g-2$ collaboration, G.W. Bennett et al., *Final Report of the Muon E821 Anomalous Magnetic Moment Measurement at BNL*, *Phys. Rev.* **D 73** (2006) 072003 [hep-ex/0602035] [INSPIRE].

[2] M. Davier, A. Hoecker, B. Malaescu and Z. Zhang, *Reevaluation of the Hadronic Contributions to the Muon g-2 and to alpha(MZ)*, *Eur. Phys. J.* **C 71** (2011) 1515 [*Erratum ibid.* **C 72** (2012) 1874] [arXiv:1010.4180] [INSPIRE].

[3] K. Hagiwara, R. Liao, A.D. Martin, D. Nomura and T. Teubner, $(g-2)_\mu$ *and* $\alpha(M_Z^2)$ *re-evaluated using new precise data*, *J. Phys.* **G 38** (2011) 085003 [arXiv:1105.3149] [INSPIRE].

[4] F. Jegerlehner and A. Nyffeler, *The muon* $g-2$, *Phys. Rept.* **477** (2009) 1 [arXiv:0902.3360] [INSPIRE].

[5] Muon $g-2$ collaboration, J. Grange et al., *Muon* $(g-2)$ *Technical Design Report*, arXiv:1501.06858 [INSPIRE].

[6] J-PARC muon $g-2$/EDM collaboration, H. Iinuma, *New approach to the muon* $g-2$ *and EDM experiment at J-PARC*, *J. Phys. Conf. Ser.* **295** (2011) 012032 [INSPIRE].

[7] J. Cao, P. Wan, L. Wu and J.M. Yang, *Lepton-Specific Two-Higgs Doublet Model: Experimental Constraints and Implication on Higgs Phenomenology*, *Phys. Rev.* **D 80** (2009) 071701 [arXiv:0909.5148] [INSPIRE].

[8] A. Broggio, E.J. Chun, M. Passera, K.M. Patel and S.K. Vempati, *Limiting two-Higgs-doublet models*, *JHEP* **11** (2014) 058 [arXiv:1409.3199] [INSPIRE].

[9] L. Wang and X.-F. Han, *A light pseudoscalar of 2HDM confronted with muon* $g-2$ *and experimental constraints*, *JHEP* **05** (2015) 039 [arXiv:1412.4874] [INSPIRE].

[10] V.D. Barger, J.L. Hewett and R.J.N. Phillips, *New Constraints on the Charged Higgs Sector in Two Higgs Doublet Models*, *Phys. Rev.* **D 41** (1990) 3421 [INSPIRE].

[11] Y. Grossman, *Phenomenology of models with more than two Higgs doublets*, *Nucl. Phys.* **B 426** (1994) 355 [hep-ph/9401311] [INSPIRE].

[12] M. Aoki, S. Kanemura, K. Tsumura and K. Yagyu, *Models of Yukawa interaction in the two Higgs doublet model and their collider phenomenology*, *Phys. Rev.* **D 80** (2009) 015017 [arXiv:0902.4665] [INSPIRE].

[13] S.L. Glashow and S. Weinberg, *Natural Conservation Laws for Neutral Currents*, *Phys. Rev.* **D 15** (1977) 1958 [INSPIRE].

[14] Y. Omura, E. Senaha and K. Tobe, *Lepton-flavor-violating Higgs decay* $h \to \mu\tau$ *and muon anomalous magnetic moment in a general two Higgs doublet model*, *JHEP* **05** (2015) 028 [arXiv:1502.07824] [INSPIRE].

[15] T. Han, S.K. Kang and J. Sayre, *Muon* $g-2$ *in the aligned two Higgs doublet model*, *JHEP* **02** (2016) 097 [arXiv:1511.05162] [INSPIRE].

JHEP07(2017)012

[16] Y. Omura, E. Senaha and K. Tobe, *τ- and μ-physics in a general two Higgs doublet model with $\mu - \tau$ flavor violation*, *Phys. Rev.* **D 94** (2016) 055019 [arXiv:1511.08880] [INSPIRE].

[17] T. Abe, R. Sato and K. Yagyu, *Lepton-specific two Higgs doublet model as a solution of muon $g-2$ anomaly*, *JHEP* **07** (2015) 064 [arXiv:1504.07059] [INSPIRE].

[18] E.J. Chun and J. Kim, *Leptonic Precision Test of Leptophilic Two-Higgs-Doublet Model*, *JHEP* **07** (2016) 110 [arXiv:1605.06298] [INSPIRE].

[19] J.F. Gunion and H.E. Haber, *The CP conserving two Higgs doublet model: The approach to the decoupling limit*, *Phys. Rev.* **D 67** (2003) 075019 [hep-ph/0207010] [INSPIRE].

[20] ATLAS, CMS collaborations, *Measurements of the Higgs boson production and decay rates and constraints on its couplings from a combined ATLAS and CMS analysis of the LHC pp collision data at $\sqrt{s} = 7$ and 8 TeV*, *JHEP* **08** (2016) 045 [arXiv:1606.02266] [INSPIRE].

[21] A. Dedes and H.E. Haber, *Can the Higgs sector contribute significantly to the muon anomalous magnetic moment?*, *JHEP* **05** (2001) 006 [hep-ph/0102297] [INSPIRE].

[22] J.D. Bjorken and S. Weinberg, *A Mechanism for Nonconservation of Muon Number*, *Phys. Rev. Lett.* **38** (1977) 622 [INSPIRE].

[23] S.M. Barr and A. Zee, *Electric Dipole Moment of the Electron and of the Neutron*, *Phys. Rev. Lett.* **65** (1990) 21 [*Erratum ibid.* **65** (1990) 2920] [INSPIRE].

[24] N.G. Deshpande and E. Ma, *Pattern of Symmetry Breaking with Two Higgs Doublets*, *Phys. Rev.* **D 18** (1978) 2574 [INSPIRE].

[25] K.G. Klimenko, *On Necessary and Sufficient Conditions for Some Higgs Potentials to Be Bounded From Below*, *Theor. Math. Phys.* **62** (1985) 58 [INSPIRE].

[26] M. Sher, *Electroweak Higgs Potentials and Vacuum Stability*, *Phys. Rept.* **179** (1989) 273 [INSPIRE].

[27] S. Nie and M. Sher, *Vacuum stability bounds in the two Higgs doublet model*, *Phys. Lett.* **B 449** (1999) 89 [hep-ph/9811234] [INSPIRE].

[28] S. Kanemura, T. Kasai and Y. Okada, *Mass bounds of the lightest CP even Higgs boson in the two Higgs doublet model*, *Phys. Lett.* **B 471** (1999) 182 [hep-ph/9903289] [INSPIRE].

[29] S. Kanemura, T. Kubota and E. Takasugi, *Lee-Quigg-Thacker bounds for Higgs boson masses in a two doublet model*, *Phys. Lett.* **B 313** (1993) 155 [hep-ph/9303263] [INSPIRE].

[30] A.G. Akeroyd, A. Arhrib and E.-M. Naimi, *Note on tree level unitarity in the general two Higgs doublet model*, *Phys. Lett.* **B 490** (2000) 119 [hep-ph/0006035] [INSPIRE].

[31] I.F. Ginzburg and I.P. Ivanov, *Tree-level unitarity constraints in the most general 2HDM*, *Phys. Rev.* **D 72** (2005) 115010 [hep-ph/0508020] [INSPIRE].

[32] S. Kanemura and K. Yagyu, *Unitarity bound in the most general two Higgs doublet model*, *Phys. Lett.* **B 751** (2015) 289 [arXiv:1509.06060] [INSPIRE].

[33] F. Staub, *SARAH 4: A tool for (not only SUSY) model builders*, *Comput. Phys. Commun.* **185** (2014) 1773 [arXiv:1309.7223] [INSPIRE].

[34] Heavy Flavor Averaging Group (HFAG) collaboration, Y. Amhis et al., *Averages of b-hadron, c-hadron and τ-lepton properties as of summer 2014*, arXiv:1412.7515 [INSPIRE].

[35] M.E. Peskin and T. Takeuchi, *A new constraint on a strongly interacting Higgs sector*, *Phys. Rev. Lett.* **65** (1990) 964 [INSPIRE].

JHEP07(2017)012

[36] M.E. Peskin and T. Takeuchi, *Estimation of oblique electroweak corrections*, *Phys. Rev.* **D 46** (1992) 381 [INSPIRE].

[37] C. Degrande, C. Duhr, B. Fuks, D. Grellscheid, O. Mattelaer and T. Reiter, *UFO — The Universal FeynRules Output*, *Comput. Phys. Commun.* **183** (2012) 1201 [arXiv:1108.2040] [INSPIRE].

[38] A. Alloul, N.D. Christensen, C. Degrande, C. Duhr and B. Fuks, *FeynRules 2.0 — A complete toolbox for tree-level phenomenology*, *Comput. Phys. Commun.* **185** (2014) 2250 [arXiv:1310.1921] [INSPIRE].

[39] J. Alwall, M. Herquet, F. Maltoni, O. Mattelaer and T. Stelzer, *MadGraph 5: Going Beyond*, *JHEP* **06** (2011) 128 [arXiv:1106.0522] [INSPIRE].

[40] CMS collaboration, *Search for evidence of Type-III seesaw mechanism in multilepton final states in pp collisions at* $\sqrt{s} = 13$ *TeV*, CMS-PAS-EXO-17-006.

[41] T. Sjöstrand, S. Mrenna and P.Z. Skands, *PYTHIA 6.4 Physics and Manual*, *JHEP* **05** (2006) 026 [hep-ph/0603175] [INSPIRE].

[42] DELPHES 3 collaboration, J. de Favereau et al., *DELPHES 3, A modular framework for fast simulation of a generic collider experiment*, *JHEP* **02** (2014) 057 [arXiv:1307.6346] [INSPIRE].

[43] T. Junk, *Confidence level computation for combining searches with small statistics*, *Nucl. Instrum. Meth.* **A 434** (1999) 435 [hep-ex/9902006] [INSPIRE].

[44] A.L. Read, *Modified frequentist analysis of search results (The CL(s) method)*, in proceedings of *Workshop on Confidence Limits*, Geneva, Switzerland (2000) [INSPIRE].

[45] A.L. Read, *Presentation of search results: The CL(s) technique*, *J. Phys.* **G 28** (2002) 2693 [INSPIRE].

[46] J. Mrazek, A. Pomarol, R. Rattazzi, M. Redi, J. Serra and A. Wulzer, *The Other Natural Two Higgs Doublet Model*, *Nucl. Phys.* **B 853** (2011) 1 [arXiv:1105.5403] [INSPIRE].

[47] S. De Curtis, S. Moretti, K. Yagyu and E. Yildirim, *Perturbative unitarity bounds in composite two-Higgs doublet models*, *Phys. Rev.* **D 94** (2016) 055017 [arXiv:1602.06437] [INSPIRE].

[48] S. De Curtis, S. Moretti, K. Yagyu and E. Yildirim, *LHC Phenomenology of Composite 2-Higgs Doublet Models*, arXiv:1610.02687 [INSPIRE].

[49] Particle Data Group collaboration, C. Patrignani et al., *Review of Particle Physics*, *Chin. Phys.* **C 40** (2016) 100001 [INSPIRE].

[50] I. Maksymyk, C.P. Burgess and D. London, *Beyond S, T and U*, *Phys. Rev.* **D 50** (1994) 529 [hep-ph/9306267] [INSPIRE].

[51] C.P. Burgess, S. Godfrey, H. Konig, D. London and I. Maksymyk, *A Global fit to extended oblique parameters*, *Phys. Lett.* **B 326** (1994) 276 [hep-ph/9307337] [INSPIRE].

[52] T. Hahn and M. Pérez-Victoria, *Automatized one loop calculations in four-dimensions and D-dimensions*, *Comput. Phys. Commun.* **118** (1999) 153 [hep-ph/9807565] [INSPIRE].

JHEP07(2017)012